Development of a quantitative model for light-excited tunneling

This content is part of the PhD thesis of Michael Schnedler

Full thesis available under ISBN: 978-3-95806-075-3

Chapter 1

Development of a quantitative model for light-excited tunneling

1.1 The tunnel current model

Eq. 1.1 equals the tunnel current density equation given by Ref. [1] with a negative density-of-states effective mass $\alpha = m_{\mathrm{eff,V}}/m_{\mathrm{e}}$ of the valence band.

$$J_{\mathrm{V}} = -\frac{m_{\mathrm{e}}e}{2\pi^2\hbar^3}\int_{E_{\mathrm{F,tip}}}^{E_{\mathrm{F}}} dE\Theta\left(E_{\mathrm{V}}-E\right)\int_{E}^{E+\alpha[E_{\mathrm{V}}-E]} dW D(W) \tag{1.1}$$

In analogy, the tunnel current density for tunneling into empty conduction band states is given by[1]

$$J_{\mathrm{C}} = -\frac{m_{\mathrm{e}}e}{2\pi^2\hbar^3}\int_{E_{\mathrm{F,tip}}}^{E_{\mathrm{F}}} dE\Theta\left(E-E_{\mathrm{C}}\right)\int_{E}^{E+\alpha'[E_{\mathrm{C}}-E]} dW D(W) \tag{1.2}$$

with $\alpha' = m_{\mathrm{eff,C}}/m_{\mathrm{e}}$ being the density-of-states effective mass of the conduction band $m_{\mathrm{eff,C}}$, divided by the electron rest mass. Note, this standard model is extended by quasi-Fermi energies and quasi-effective masses later, in order to account for light-excited carrier concentrations.

1.1.1 The transmission coefficient

Transmission through vacuum

The transmission coefficient $D(W)$, mainly determined by the WKB approximation, is introduced as the integral over the barrier region $x = [-a, a]$[1]

$$D(W) = \exp\left(-2\int_{-a}^{a} |k_\mathrm{x}|\, dx\right) \tag{1.3}$$

where the normal energy is $W = E - \hbar^2\vec{k}_\parallel^2/(2m_\mathrm{e})$ and the normal wave vector is $k_\mathrm{x}^2 = (2m_\mathrm{e})/\hbar^2\,(V-E) + |\vec{k}_\parallel|^2$. From this, one obtains the following equation for the transmission coefficient.[2]

$$D(W) = \exp\left(-2\int_{-a}^{a} \sqrt{\frac{2m_\mathrm{e}}{\hbar^2}\,(V-W)}dx\right) \tag{1.4}$$

The shape of the potential through the central axis of the tip apex $V(x)$ is defined by the solution of the Poisson equation for the electrostatic potential between the tip and the semiconductor, as will be discussed later.

1.2 Solution of Poisson and continutiy equations

This section is taken partially from Ref. [13] and from my PhD-thesis (ISBN: 978-3-95806-075-3, Forschungszentrum Jülich GmbH Zentralbibliothek, Verlag Jülich (2015), http://hdl.handle.net/2128/9188).

1.3 Electrostatic potential and carrier distribution

The calculation of the tunnel current requires the electrostatic potential distribution for a biased metal tip-vacuum-semiconductor system. This system requires a full three-dimensional solution of the Poisson equation, since a one-dimensional analytical solution does not consider the effect of the localized shape of the tip on the electrostatic potential. In this section the approach used for calculating the electrostatic potential and charge carrier distributions is described. The latter ones

are required for a quantitative derivation of the tunnel current under irradiation conditions since generation and recombination terms are introduced, which allow the treatment of additional light excited charge carriers.

1.3.1 Carrier concentration in parabolic band approximation

The charge density $\rho(u)$ of the a semiconductor is given by

$$\rho(u) = e\left(N_{\mathrm{D}}^{+} - N_{\mathrm{A}}^{-} + p_0 - n_0\right) \tag{1.5}$$

where n_0 is the concentration of free electrons and p_0 is the concentration of free holes. These charge densities in the semiconductor are assumed to follow the effective mass approximations. For the conduction band, this approximation is given by[9]

$$n_0 = N_{\mathrm{C}} \frac{2}{\sqrt{\pi}} F_{1/2}\left(\frac{E_{\mathrm{F}} - E_{\mathrm{C}}}{kT}\right) \tag{1.6}$$

where E_{C} is the minimum of the conduction band and $F_{1/2}$ is the Fermi-Dirac integral (as defined below). N_{C} is the effective density of states, given by $N_{\mathrm{C}} = 2(2\pi m_{\mathrm{eff,C}} kT/h^2)^{3/2}$. For the charge density of the valence band, the approximation is given by

$$p_0 = N_{\mathrm{V}} \frac{2}{\sqrt{\pi}} F_{1/2}\left(\frac{E_{\mathrm{V}} - E_{\mathrm{F}}}{kT}\right) \tag{1.7}$$

where E_{V} is the maximum of the valence band and $N_{\mathrm{V}} = 2(2\pi m_{\mathrm{eff,V}} kT/h^2)^{3/2}$.

The density of ionized donors N_{D}^{+} and acceptors N_{A}^{-} are defined as [7]

$$N_{\mathrm{D}}^{+} = N_{\mathrm{D}}\left(1 + 2\exp\left[\left(E_{\mathrm{F}} - E_{\mathrm{D}}\right)/kT\right]\right)^{-1} \tag{1.8}$$

$$N_{\mathrm{A}}^{-} = N_{\mathrm{A}}\left(1 + 2\exp\left[\left(E_{\mathrm{A}} - E_{\mathrm{F}}\right)/kT\right]\right)^{-1} \tag{1.9}$$

respectively, where N_{D} (N_{A}) is the concentration of donors (acceptors) and E_{D} (E_{A}) is the respective energy level.

The Fermi-Dirac integral $F_{\mathrm{j}}(\eta)$ is defined by:[7]

$$F_{\mathrm{j}}(\eta) = \int_0^{\infty} \frac{x^j}{1 + \exp(x - \eta)} dx \tag{1.10}$$

Equation 1.10 is charaterized by the absence of the prefactor $1/\Gamma(j+1)$, where $\Gamma(j)$ is the Gamma function, and is also known as Sommerfeld's definition of the

Fermi-Dirac integral.[10] Further, the derivative of the Fermi-Dirac integral with respect to η yields a decrementation of j by minus one:[10]

$$\frac{d}{d\eta}F_{\mathrm{j}}(\eta) = F_{\mathrm{j\text{-}1}}(\eta) \tag{1.11}$$

1.3.2 System of differential equations

Thus far, Feenstra solved this kind of electrostatic problem using a finite difference method to iteratively solve the Poisson equation.[6] The charge densities n_0 and p_0 in the semiconductor are assumed to follow the effective mass approximations, as in Eqs. 1.6 and 1.7. Besides some material properties and the temperature, which is assumed to be constant, the electron and hole densities in the effective mass approximation depend only on the position of the valence and conduction band edges relative to the Fermi energy. Hence, these equations do not hold for the description of additional excess carriers generated by photon interaction.

Thus, here the continuity equations for electrons and holes are introduced, additionally. This will give a more general description of the problem, enabling the introduction of carrier generation and recombination. Overall, it is necessary to solve three coupled partial differential equations:

The Poisson equation for the electrostatic potential $\phi(x, y, z)$ at the position (x, y, z) is given by

$$\Delta\phi(x, y, z) + \frac{e}{\epsilon_0\epsilon_{\mathrm{r}}}\left(p(x, y, z) - n(x, y, z) + N_{\mathrm{D}}^{+} - N_{\mathrm{A}}^{-}\right) = 0 \tag{1.12}$$

where $n(x, y, z)$ and $p(x, y, z)$ are the electron and hole concentrations at position (x, y, z), respectively. The density of ionized donors N_{D}^{+} and acceptors N_{A}^{-} are defined as in Eqs. 1.8 and 1.9.

Assuming a time-invariant charge distribution, the continuity equations for electrons and holes are

$$\nabla \cdot \vec{J}_{\mathrm{n}} - e \cdot R = 0 \tag{1.13}$$

$$\nabla \cdot \vec{J}_{\mathrm{p}} + e \cdot R = 0 \tag{1.14}$$

where R is a time-averaged generation or recombination rate and $\vec{J}_{\mathrm{n}}$ ($\vec{J}_{\mathrm{p}}$) is the current density for electrons (holes). $\vec{J}_{\mathrm{n}}$ and $\vec{J}_{\mathrm{p}}$ can be separated into drift and diffusion terms: [14]

$$\vec{J}_{\mathrm{n}} = e\left(\mu_{\mathrm{n}} n(x, y, z)\vec{E} + D_{\mathrm{n}}\nabla n(x, y, z)\right) \tag{1.15}$$

$$\vec{J}_{\mathrm{p}} = e\left(\mu_{\mathrm{p}} p(x,y,z)\vec{E} - D_{\mathrm{p}}\nabla p(x,y,z)\right) \tag{1.16}$$

where μ_{n} (μ_{p}) is the mobility and D_{n} (D_{p}) is the diffusion coefficient of electrons (holes) in the semiconductor. D_{n} (D_{p}) is connected to μ_{n} (μ_{p}) by the Einstein relation. Note, the mobility (and the diffusion coefficient) is assumed to be location-independent in this calculation. Inserting Eqs. 1.15 and 1.16 into Eqs. 1.13 and 1.14, respectively, and using the relation $\vec{E} = -\nabla\phi$, the continuity equations become

$$\nabla \cdot (D_{\mathrm{n}} \cdot \nabla n(x,y,z) - \mu_{\mathrm{n}} n(x,y,z) \cdot \nabla\phi) - R = 0 \tag{1.17}$$

$$\nabla \cdot (D_{\mathrm{p}} \cdot \nabla p(x,y,z) + \mu_{\mathrm{p}} p(x,y,z) \cdot \nabla\phi) - R = 0 \tag{1.18}$$

1.3.3 Difference equations

Equations 1.12, 1.17, and 1.18 represent a system of three coupled partial differential equations which cannot be solved analytically in full generality.[14] For numerical computations one needs adequate *difference* equations for these *differential* equations. In analogy to Selberherr's discretization approach,[14] the differential operators are directly replaced by their corresponding difference operators. The derivation of the discretized Poisson equation replacing Eq. 1.12 is strait forward since the Laplace operator has to be replaced, only. One divides the three spatial directions into a mesh of discrete points (which are in general not equidistant). The continuous physical coordinates (x, y, z) become discrete indices (i, j, k), which are mapped to discrete physical coordinates $(x_{\mathrm{i}}, y_{\mathrm{j}}, z_{\mathrm{k}})$. Hence, for an arbitrary function $f(x_{\mathrm{i}}, y_{\mathrm{j}}, z_{\mathrm{k}})$, the abbreviated notation $f_{\mathrm{i,j,k}}$ is used. Furthermore, according to Fig. 1.1, it is $f_{\mathrm{i+1/2,j,k}} = f([x_{\mathrm{i}} + x_{\mathrm{i+1}}]/2, y_{\mathrm{j}}, z_{\mathrm{k}})$.[14] From Fig. 1.1 one can also obtain the second partial derivative of f along, e.g., the x direction:

$$\left.\frac{\partial^2 f}{\partial x^2}\right|_{\mathrm{i,j,k}} \approx \frac{\left.\frac{\partial f}{\partial x}\right|_{\mathrm{i+1/2,j,k}} - \left.\frac{\partial f}{\partial x}\right|_{\mathrm{i\text{-}1/2,j,k}}}{(x_{\mathrm{i+1}} - x_{\mathrm{i\text{-}1}})/2} \tag{1.19}$$

The first partial derivatives at the mid-interval positions $i + 1/2$ and $i - 1/2$ are given by[14]

$$\left.\frac{\partial f}{\partial x}\right|_{\mathrm{i+1/2,j,k}} \approx \frac{f_{\mathrm{i+1,j,k}} - f_{\mathrm{i,j,k}}}{x_{\mathrm{i+1}} - x_{\mathrm{i}}} \tag{1.20}$$

$$\left.\frac{\partial f}{\partial x}\right|_{\mathrm{i\text{-}1/2,j,k}} \approx \frac{f_{\mathrm{i,j,k}} - f_{\mathrm{i\text{-}1,j,k}}}{x_{\mathrm{i}} - x_{\mathrm{i\text{-}1}}} \tag{1.21}$$

With the help of Eqs. 1.19, 1.20 and 1.21, the Laplace operator in Eq. 1.12 can be approximated by[14]

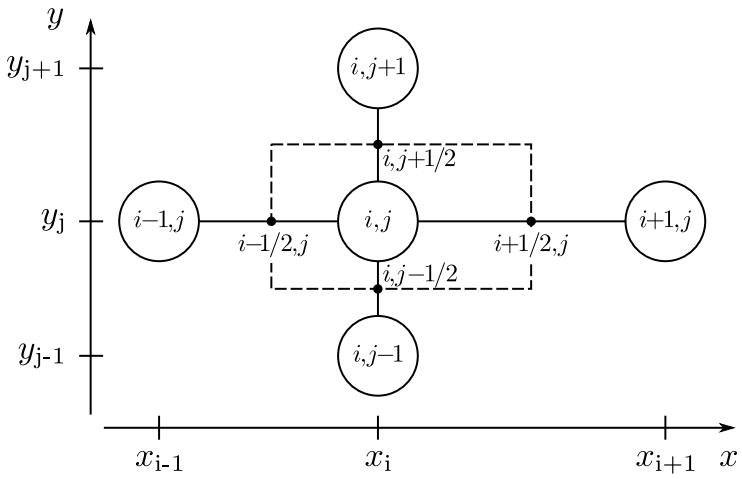

Figure 1.1: Sketch of the finite difference grid in two dimensions for reasons of clarification, in analogy to Ref. [14]

$$\left(\frac{\frac{\phi_{i+1,j,k}-\phi_{i,j,k}}{x_{i+1}-x_i} - \frac{\phi_{i,j,k}-\phi_{i-1,j,k}}{x_i-x_{i-1}}}{\frac{x_{i+1}-x_{i-1}}{2}} + \frac{\frac{\phi_{i,j+1,k}-\phi_{i,j,k}}{y_{j+1}-y_j} - \frac{\phi_{i,j,k}-\phi_{i,j-1,k}}{y_j-y_{j-1}}}{\frac{y_{j+1}-y_{j-1}}{2}} + \frac{\frac{\phi_{i,j,k+1}-\phi_{i,j,k}}{z_{k+1}-z_k} - \frac{\phi_{i,j,k}-\phi_{i,j,k-1}}{z_k-z_{k-1}}}{\frac{z_{k+1}-z_{k-1}}{2}} \right) + \frac{e}{\epsilon_0 \epsilon_r} \left(-n_{i,j,k} + p_{i,j,k} + N_D^+ - N_A^- \right) = 0 \tag{1.22}$$

The derivation of the discretized continuity equations for holes and electrons is more complex and is derived in analogy to Ref. [14] (starting on page 155) for the three dimensional case here. The resulting discretized continuity equation for electrons

is

$$
\begin{aligned}
&\frac{B\left(\frac{\phi_{\mathrm{i+1,j,k}}-\phi_{\mathrm{i,j,k}}}{kT}\right)\cdot n_{\mathrm{i+1,j,k}} - B\left(\frac{\phi_{\mathrm{i,j,k}}-\phi_{\mathrm{i+1,j,k}}}{kT}\right)\cdot n_{\mathrm{i,j,k}}}{(x_{\mathrm{i+1}}-x_{\mathrm{i}})\cdot\frac{x_{\mathrm{i+1}}-x_{\mathrm{i\text{-}1}}}{2}} \\
-&\frac{B\left(\frac{\phi_{\mathrm{i,j,k}}-\phi_{\mathrm{i\text{-}1,j,k}}}{kT}\right)\cdot n_{\mathrm{i,j,k}} - B\left(\frac{\phi_{\mathrm{i\text{-}1,j,k}}-\phi_{\mathrm{i,j,k}}}{kT}\right)\cdot n_{\mathrm{i\text{-}1,j,k}}}{(x_{\mathrm{i}}-x_{\mathrm{i\text{-}1}})\cdot\frac{x_{\mathrm{i+1}}-x_{\mathrm{i\text{-}1}}}{2}} \\
+&\frac{B\left(\frac{\phi_{\mathrm{i,j+1,k}}-\phi_{\mathrm{i,j,k}}}{kT}\right)\cdot n_{\mathrm{i,j+1,k}} - B\left(\frac{\phi_{\mathrm{i,j,k}}-\phi_{\mathrm{i,j+1,k}}}{kT}\right)\cdot n_{\mathrm{i,j,k}}}{(y_{\mathrm{j+1}}-y_{\mathrm{j}})\cdot\frac{y_{\mathrm{j+1}}-y_{\mathrm{j\text{-}1}}}{2}} \\
-&\frac{B\left(\frac{\phi_{\mathrm{i,j,k}}-\phi_{\mathrm{i,j\text{-}1,k}}}{kT}\right)\cdot n_{\mathrm{i,j,k}} - B\left(\frac{\phi_{\mathrm{i,j\text{-}1,k}}-\phi_{\mathrm{i,j,k}}}{kT}\right)\cdot n_{\mathrm{i,j\text{-}1,k}}}{(y_{\mathrm{j}}-y_{\mathrm{j\text{-}1}})\cdot\frac{y_{\mathrm{j+1}}-y_{\mathrm{j\text{-}1}}}{2}} \\
+&\frac{B\left(\frac{\phi_{\mathrm{i,j,k+1}}-\phi_{\mathrm{i,j,k}}}{kT}\right)\cdot n_{\mathrm{i,j,k+1}} - B\left(\frac{\phi_{\mathrm{i,j,k}}-\phi_{\mathrm{i,j,k+1}}}{kT}\right)\cdot n_{\mathrm{i,j,k}}}{(z_{\mathrm{k+1}}-z_{\mathrm{k}})\cdot\frac{z_{\mathrm{k+1}}-z_{\mathrm{k\text{-}1}}}{2}} \\
-&\frac{B\left(\frac{\phi_{\mathrm{i,j,k}}-\phi_{\mathrm{i,j,k\text{-}1}}}{kT}\right)\cdot n_{\mathrm{i,j,k}} - B\left(\frac{\phi_{\mathrm{i,j,k\text{-}1}}-\phi_{\mathrm{i,j,k}}}{kT}\right)\cdot n_{\mathrm{i,j,k\text{-}1}}}{(z_{\mathrm{k}}-z_{\mathrm{k\text{-}1}})\cdot\frac{z_{\mathrm{k+1}}-z_{\mathrm{k\text{-}1}}}{2}} \\
-&\frac{R}{D_{\mathrm{n}}} = 0
\end{aligned}
\tag{1.23}
$$

with the Bernoulli function $B(x) = x/(\exp(x) - 1)$.

Analogously, the discretized continuity equation for holes can be found to be [14]

$$\begin{aligned}
&\frac{B\left(\frac{\phi_{\mathrm{i,j,k}}-\phi_{\mathrm{i+1,j,k}}}{kT}\right)\cdot p_{\mathrm{i+1,j,k}} - B\left(\frac{\phi_{\mathrm{i+1,j,k}}-\phi_{\mathrm{i,j,k}}}{kT}\right)\cdot p_{\mathrm{i,j,k}}}{(x_{\mathrm{i+1}}-x_{\mathrm{i}})\cdot\frac{x_{\mathrm{i+1}}-x_{\mathrm{i\text{-}1}}}{2}} \\
-&\frac{B\left(\frac{\phi_{\mathrm{i\text{-}1,j,k}}-\phi_{\mathrm{i,j,k}}}{kT}\right)\cdot p_{\mathrm{i,j,k}} - B\left(\frac{\phi_{\mathrm{i,j,k}}-\phi_{\mathrm{i\text{-}1,j,k}}}{kT}\right)\cdot p_{\mathrm{i\text{-}1,j,k}}}{(x_{\mathrm{i}}-x_{\mathrm{i\text{-}1}})\cdot\frac{x_{\mathrm{i+1}}-x_{\mathrm{i\text{-}1}}}{2}} \\
+&\frac{B\left(\frac{\phi_{\mathrm{i,j,k}}-\phi_{\mathrm{i,j+1,k}}}{kT}\right)\cdot p_{\mathrm{i,j+1,k}} - B\left(\frac{\phi_{\mathrm{i,j+1,k}}-\phi_{\mathrm{i,j,k}}}{kT}\right)\cdot p_{\mathrm{i,j,k}}}{(y_{\mathrm{j+1}}-y_{\mathrm{j}})\cdot\frac{y_{\mathrm{j+1}}-y_{\mathrm{j\text{-}1}}}{2}} \\
-&\frac{B\left(\frac{\phi_{\mathrm{i,j\text{-}1,k}}-\phi_{\mathrm{i,j,k}}}{kT}\right)\cdot p_{\mathrm{i,j,k}} - B\left(\frac{\phi_{\mathrm{i,j,k}}-\phi_{\mathrm{i,j\text{-}1,k}}}{kT}\right)\cdot p_{\mathrm{i,j\text{-}1,k}}}{(y_{\mathrm{j}}-y_{\mathrm{j\text{-}1}})\cdot\frac{y_{\mathrm{j+1}}-y_{\mathrm{j\text{-}1}}}{2}} \\
+&\frac{B\left(\frac{\phi_{\mathrm{i,j,k}}-\phi_{\mathrm{i,j,k+1}}}{kT}\right)\cdot p_{\mathrm{i,j,k+1}} - B\left(\frac{\phi_{\mathrm{i,j,k+1}}-\phi_{\mathrm{i,j,k}}}{kT}\right)\cdot p_{\mathrm{i,j,k}}}{(z_{\mathrm{k+1}}-z_{\mathrm{k}})\cdot\frac{z_{\mathrm{k+1}}-z_{\mathrm{k\text{-}1}}}{2}} \\
-&\frac{B\left(\frac{\phi_{\mathrm{i,j,k\text{-}1}}-\phi_{\mathrm{i,j,k}}}{kT}\right)\cdot p_{\mathrm{i,j,k}} - B\left(\frac{\phi_{\mathrm{i,j,k}}-\phi_{\mathrm{i,j,k\text{-}1}}}{kT}\right)\cdot p_{\mathrm{i,j,k\text{-}1}}}{(z_{\mathrm{k}}-z_{\mathrm{k\text{-}1}})\cdot\frac{z_{\mathrm{k+1}}-z_{\mathrm{k\text{-}1}}}{2}} \\
-&\frac{R}{D_{\mathrm{p}}} = 0
\end{aligned} \tag{1.24}$$

1.3.4 Boundaries and interfaces

Neumann boundary conditions are assumed for both the electrostatic potential and the charge densities. This means that at the borders of the calculation grid in normal direction the partial derivation of the electrostatic potential and the current densities for electrons and holes are zero. A precise derivation of the boundary conditions with respect to a minimization of the truncation error is given in Ref. [14] on page 172. Particular attention must be paid to the continuity condition for the electrostatic potential at the surface of the semiconductor. For a surface, which is nearly free of surface states, the normal component of the electric displacement field $\vec{D}$ remains constant at the transition from the semiconductor to the vacuum. With surface states being present within or even outside of the fundamental band gap, a surface charge distribution σ gives rise to a change of $\vec{D}$ according to Eq. 1.25.

$$\vec{n}\cdot(\vec{D}_{\mathrm{vac}} - \vec{D}_{\mathrm{semi}}) = \sigma \tag{1.25}$$

where $\vec{n}$ is the normal vector of the surface. Using the relation for isotropic media $\vec{D} = -\epsilon_0\epsilon_\mathrm{r} \cdot \nabla\phi$ one obtains for a normal vector in x-direction:

$$\epsilon_0\epsilon_\mathrm{r} \cdot \left.\frac{\partial\phi}{\partial x}\right|_\mathrm{semi} - \epsilon_0 \left.\frac{\partial\phi}{\partial x}\right|_\mathrm{vac} - \sigma = 0 \tag{1.26}$$

Again, Eq. 1.26 can be discretized by employing difference operators.[14] Assuming that all points $x \geq x_\mathrm{surf}$ belong to the semiconductor, whereas all points $x < x_\mathrm{surf}$ belong to either the tip or the vacuum, Eq. 1.22 needs to be replaced for $x = x_\mathrm{surf}$ (or $i = i_\mathrm{surf}$, respectively) by

$$\begin{aligned}
&\left(\frac{\epsilon_\mathrm{r}\epsilon_0 \dfrac{\phi_{\mathrm{i+1,j,k}} - \phi_{\mathrm{i,j,k}}}{x_{\mathrm{i+1}} - x_\mathrm{i}} - \epsilon_0 \dfrac{\phi_{\mathrm{i,j,k}} - \phi_{\mathrm{i\text{-}1,j,k}}}{x_\mathrm{i} - x_{\mathrm{i\text{-}1}}} + \sigma_{\mathrm{i,j,k}}}{\dfrac{\epsilon_\mathrm{r}\epsilon_0 \left(x_{\mathrm{i+1}} - x_\mathrm{i}\right) + \epsilon_0 \left(x_\mathrm{i} - x_{\mathrm{i\text{-}1}}\right)}{2}} \right. \\
&\left. + \frac{\dfrac{\phi_{\mathrm{i,j+1,k}} - \phi_{\mathrm{i,j,k}}}{y_{\mathrm{j+1}} - y_\mathrm{j}} - \dfrac{\phi_{\mathrm{i,j,k}} - \phi_{\mathrm{i,j\text{-}1,k}}}{y_\mathrm{j} - y_{\mathrm{j\text{-}1}}}}{\dfrac{y_{\mathrm{j+1}} - y_{\mathrm{j\text{-}1}}}{2}} + \frac{\dfrac{\phi_{\mathrm{i,j,k+1}} - \phi_{\mathrm{i,j,k}}}{z_{\mathrm{k+1}} - z_\mathrm{k}} - \dfrac{\phi_{\mathrm{i,j,k}} - \phi_{\mathrm{i,j,k\text{-}1}}}{z_\mathrm{k} - z_{\mathrm{k\text{-}1}}}}{\dfrac{z_{\mathrm{k+1}} - x_{\mathrm{k\text{-}1}}}{2}} \right) \\
&- \frac{e}{\epsilon_0\epsilon_\mathrm{r}} \frac{x_\mathrm{i} - x_{\mathrm{i\text{-}1}}}{\epsilon_\mathrm{r}\left(x_{\mathrm{i+1}} - x_\mathrm{i}\right) + \left(x_\mathrm{i} - x_{\mathrm{i\text{-}1}}\right)} \cdot \left(n_{\mathrm{i,j,k}} - p_{\mathrm{i,j,k}} - N_\mathrm{D}^+ + N_\mathrm{A}^-\right) = 0
\end{aligned} \tag{1.27}$$

In the region of the semiconductor, Eqs. 1.22 (for $x > x_\mathrm{surf}$), 1.27 (for $x = x_\mathrm{surf}$), 1.23, and 1.24 have to be solved, whereas in the region of the vacuum only Eq. 1.22 has to be solved due to the absence of charge carriers. At the tip the electrostatic potential ϕ_tip is set to a constant value, the so-called contact potential $\Delta\phi$.[15] It can be interpreted as the potential difference between the tip and the surface of the semiconductor

$$\phi_\mathrm{tip} = \Delta\phi = V + \left(E_\mathrm{F} - E_\mathrm{C} - \chi + \phi_\mathrm{m}\right)/e \tag{1.28}$$

where V is the voltage applied between the tip and the semiconductor, χ is the electron affinity of the semiconductor and ϕ_m is the work function of the tip.

1.3.5 Initial values

For the initial values of the electrostatic potential $\phi^0_{\mathrm{i,j,k}}$ and the charge densities $n^0_{\mathrm{i,j,k}}$ and $p^0_{\mathrm{i,j,k}}$ within the semiconductor, one assumes that the tip is located infinitely far away from the semiconductor's surface. Hence, the semiconductor is initialized without tip-induced band bending and with equally-distributed carrier

concentrations:

$$\left.\begin{aligned} \phi^0_{\mathrm{i,j,k}} &= 0\,\mathrm{V} \\ n^0_{\mathrm{i,j,k}} &= n_0 + c_{\mathrm{light}} \\ p^0_{\mathrm{i,j,k}} &= p_0 + c_{\mathrm{light}} \end{aligned}\right\} \text{for } i \geq i_{\mathrm{surf}} \tag{1.29}$$

n_0 and p_0 (together with E_{F}) can be easily obtained by solving the charge neutrality condition $n_0 - p_0 - N_{\mathrm{D}}^+ + N_{\mathrm{A}}^- = 0$, when the semiconductor is in equilibrium. For a sample that is illuminated by a laser beam, the initial density of the light-excited carriers c_{light} can be estimated using

$$c_{\mathrm{light}} = \alpha \cdot \frac{P_{\mathrm{opt}}}{E_{\mathrm{ph}} A_{\mathrm{light}}} \cdot \tau \tag{1.30}$$

where α is the absorption coefficient of the semiconductor, τ is the lifetime of the minority carriers, A_{light} is the illuminated surface area, P_{opt} is the optical power of the laser, and E_{ph} is the photon energy. One could also take into account that P_{opt} depends exponentially on the penetration depth of the photons. However, for the samples and light sources that were used in the experiments of this thesis (p-type GaAs with $\alpha \sim 1 \cdot 10^4 \mathrm{cm}^{-1}$ for $E_{\mathrm{ph}} = 1.58$ eV [16], see below), the change of P_{opt} in the region of interest is in the range of only a few percent and hence can be neglected.

For the given problem, one could have chosen other initial values that promise to converge faster to the optimal solution. For example, one could have estimated the tip-induced band bending within the semiconductor by the one-dimensional solution of the Poisson equation as given in Chap. **??** and use these values for $\phi^0_{\mathrm{i,j,k}}$. However, in practise, the approach given by Eq. 1.29 delivers good results.

1.3.6 Carrier generation and recombination

The generation and recombination process is modeled by radiative band-to-band transitions. For samples with direct band gaps this recombination process is taken to be dominant. The net recombination rate R_{te} in thermal equilibrium and without illumination is given by[17]

$$R_{\mathrm{te}}(x,y,z) = b \cdot (n(x,y,z) \cdot p(x,y,z) - n_0 p_0) \tag{1.31}$$

where b is the bimolecular recombination coefficient. When the laser is switched on, electron and hole pairs will be created with a rate of $R_{\mathrm{light}} = c_{\mathrm{light}}/\tau$. In the absence of the tip-induced band bending (i.e. without a potential gradient for the carriers),

a second equilibrium situation will be reached, when the net recombination rate equals R_{light}:

$$b \cdot ((n_0 + c_{\text{light}})(p_0 + c_{\text{light}}) - n_0 p_0) = R_{\text{light}} \tag{1.32}$$

With the help of Eqs. 1.30 and 1.32, b can be determined and finally, the net recombination rate R for the sample under illumination, suitable for substitution in Eqs. 1.23 and 1.24 is given by

$$R(x, y, z) = b \cdot (n(x, y, z) \cdot p(x, y, z) - n_0 p_0) - R_{\text{light}} \tag{1.33}$$

1.3.7 Numerical iteration method

The numerical iteration method used to solve Eqs. 1.22, 1.23, 1.24, and 1.27 should be discussed briefly. Although there exist many different approaches for the numerical solution of this system of nonlinear algebraic equations, it was decided to use a successive over relaxation (SOR) Newton method because of the easy implementation and the advantage that Eqs. 1.22, 1.23, and 1.24 can be sequentially used to find the solution.[14] A derivation of this and other methods in detail is for example given by Selberherr.[14] Identifying Eqs. 1.22, 1.23, and 1.24 with $F_1(\phi, n, p) = 0$, $F_2(\phi, n, p) = 0$, and $F_3(\phi, n, p) = 0$, respectively, the variation of the variables $\delta\phi^{\mathrm{k}} = \phi^{\mathrm{k+1}} - \phi^{\mathrm{k}}$, $\delta n^{\mathrm{k}} = n^{\mathrm{k+1}} - n^{\mathrm{k}}$, and $\delta p^{\mathrm{k}} = p^{\mathrm{k+1}} - p^{\mathrm{k}}$ of the k-th iteration step of the SOR Newton method are evaluated by [14]

$$\begin{aligned}
\delta\phi^{\mathrm{k,m+1}} &= -\frac{\omega \cdot F_1(\phi^{\mathrm{k}}, n^{\mathrm{k}} + \delta n^{\mathrm{k,m}}, p^{\mathrm{k}} + \delta p^{\mathrm{k,m}})}{\frac{\partial F_1^{\mathrm{k}}}{\partial \phi}} \\
\delta n^{\mathrm{k,m+1}} &= -\frac{\omega \cdot F_2(\phi^{\mathrm{k}} + \delta\phi^{\mathrm{k,m+1}}, n^{\mathrm{k}}, p^{\mathrm{k}} + \delta p^{\mathrm{k,m}})}{\frac{\partial F_2^{\mathrm{k}}}{\partial n}} \\
\delta p^{\mathrm{k,m+1}} &= -\frac{\omega \cdot F_3(\phi^{\mathrm{k}} + \delta\phi^{\mathrm{k,m+1}}, n^{\mathrm{k}} + \delta n^{\mathrm{k,m+1}}, p^{\mathrm{k}})}{\frac{\partial F_3^{\mathrm{k}}}{\partial p}}
\end{aligned} \tag{1.34}$$

where ω is a relaxation parameter. This means that an "inner" iteration (index m) has to be performed for each Newton step k.

1.3.8 Design of the mesh

In order to obtain the potential near the surface with the required spatial accuracy, rather small distances between the points of the mesh used in the finite difference

calculation are needed (in the order of 0.1 nm). However, for lower doped semiconductors the band bending may extend deep into the semiconductor (up to µm). Hence, the mesh needs to cover a volume large enough to include the full decay of the potential. In principle one could use a fully equidistant mesh, but the number of points needed would make the calculation impractical. At large distances (x, y, and z) from the semiconductor surface area facing the tip, the potential changes almost linearly and hence the points of the mesh can be increasingly separated in space. Along all three directions, equidistant points are used close to the surface area facing the tip. At larger distances, the point separation of the mesh is increased, until the mesh volume is sufficiently large. Figure 1.2(a) illustrates a three-dimensional view of a mesh similar to that used in the computations. The mesh points are located at the intersections of the lines. For the sake of clarity, the mesh consists only of one eighth of the mesh points used in the computation. Additionally, the points in the vacuum are hidden. Figure 1.2(b) represents a cross-sectional view along the central x-y plane (including mesh points in the vacuum). This mesh provides a full three-dimensional finite difference calculation, where any tip shape can be modeled. It is not limited to hyperbolically-shaped tips, as previously used.[6]

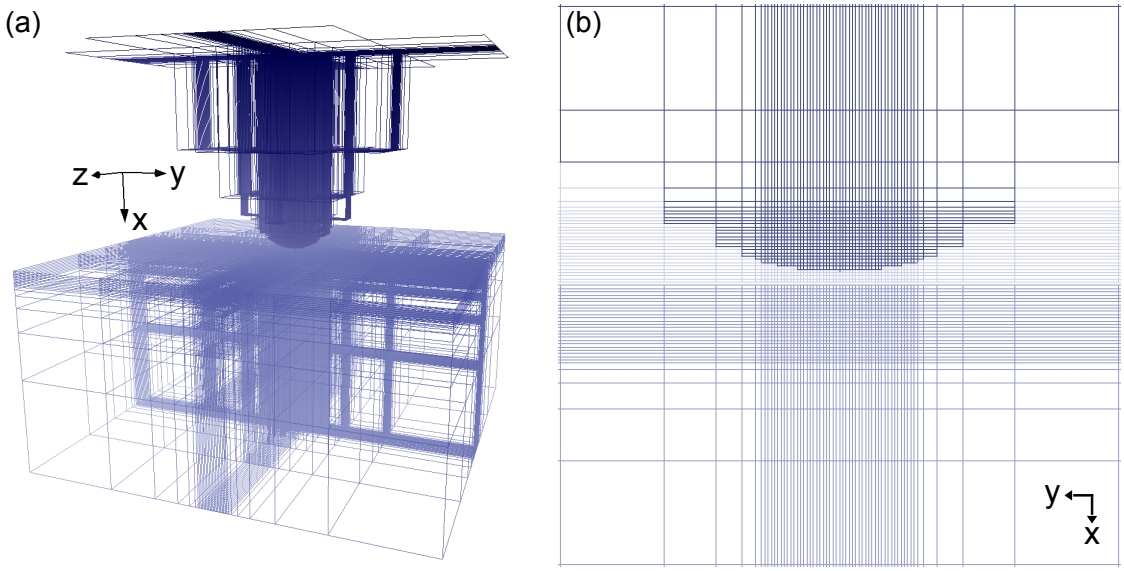

Figure 1.2: (a) Three-dimensional view of a mesh, similar to that used in the computations. The mesh points are located at the intersections of the lines. For the sake of clarity, the mesh consists only of one eighth of the mesh points used in the computation. Additionally, the points in the vacuum are hidden. (b) Cross-sectional view of the central x-y plane (isometric projection) including the mesh points in the vacuum.

1.4 Calculation of the tunnel current beyond the effective mass approximation

The calculation of the tunnel current density is based on the tunneling model presented in Sec. 1.1. The current density is given by Eqs. 1.1 and 1.2. It depends on the band edge energies, obtained from the solution of the Poisson equation, along the axis perpendicular to the sample surface (x-axis in the electrostatic calculation), through the tip apex.

These two equations cover the tunneling of electrons out of the valence band (Eq. 1.1) and out of an electron accumulation zone in the conduction band (Eq. 1.2) into the empty tip states as well as of electrons in the tip into the empty conduction band states (Eq. 1.2) or into a hole accumulation zone in the valence band (Eq. 1.1).

The total tunnel current I is the sum of all current density contributions multiplied by the tunnel area A_{tunnel}: [15]

$$I = (J_{\mathrm{V}} + J_{\mathrm{C}}) \times A_{\mathrm{tunnel}} \tag{1.35}$$

This approach assumes parabolic bands and does not incorporate the tunneling of light-excited carriers. Hence, the model is extended here in order to incorporate the concentrations of both minority and majority carriers (including light-excited carriers) obtained from the solution of the continuity equations. From these carrier concentrations the quasi Fermi levels $E_{\mathrm{FQ,C}}$ and $E_{\mathrm{FQ,V}}$ at the surface are derived. $E_{\mathrm{FQ,C}}$ ($E_{\mathrm{FQ,V}}$) is the upper (lower) limit for the energy of the electrons (holes) in the conduction band (valence band). These electrons (holes) can tunnel from the conduction band (valence band) into the tip. Hence, the quasi Fermi levels replace the upper limit of the first integral in Eqs. 1.1 and 1.2.

The quasi Fermi levels have to be determined precisely, because they affect critically the tunnel current density. Calculating the quasi Fermi levels on the basis of Eqs. 1.6 and 1.7 using the carrier densities $n(x, y, z)$ and $p(x, y, z)$ is only accurate enough for moderate carrier concentrations ($n\,(x, y, z) < N_{\mathrm{C}}$ and $p\,(x, y, z) < N_{\mathrm{V}}$), since the conduction band dispersion deviates from its parabolic approximation almost directly at E_{C}. Hence, for higher carrier concentrations one needs to integrate the calculated density of states [DOS(E)] of the investigated semiconductor (i.e. GaAs), e.g., taken from Chelikowsky and Cohen [18, 19]

$$n' = \int_{E_{\mathrm{C}}}^{\infty} dE \mathrm{DOS}(E) f_{\mathrm{S}}(E - E_{\mathrm{FQ,C}}) \tag{1.36}$$

$$p' = \int_{-\infty}^{E_\mathrm{V}} dE \mathrm{DOS}(E) f_\mathrm{S}(E_\mathrm{FQ,V} - E) \tag{1.37}$$

and numerically solve these integrals for $E_\mathrm{FQ,C}$ and $E_\mathrm{FQ,V}$, such that n' (or p') equals the carrier concentration $n(x, y, z)$ (or $p(x, y, z)$) at the surface below the tip apex. The Fermi-Dirac distribution of the semiconductor $f_\mathrm{S}(E)$ is approximated by a step function here. The same approximation is already used in the derivation of the tunnel current (Eqs. 1.1 and 1.2) and hence does not restrict the validity further.[2]

Additionally, the effective masses $m_\mathrm{eff,V}$ and $m_\mathrm{eff,C}$ of the holes and electrons, respectively, are taken to be energy-dependent. By substituting $E_\mathrm{FQ,C}$ ($E_\mathrm{FQ,V}$) and $n(x, y, z)$ ($p(x, y, z)$) into Eq. 1.6 (Eq. 1.7), it can be solved for new quasi effective masses $m_\mathrm{effq,C}$ ($m_\mathrm{effq,V}$), replacing $m_\mathrm{eff,C}$ ($m_\mathrm{eff,V}$). The resulting quasi effective masses and quasi Fermi levels are then used to calculate the tunnel current density.

Bibliography

[1] R. M. Feenstra and J. A. Stroscio, "Tunneling spectroscopy of the GaAs(110) surface," *J. Vac. Sci. Technol. B*, vol. 5, no. 4, pp. 923–929, 1987.

[2] J. Bono and R. H. Good, "Theoretical discussion of the scanning tunneling microscope applied to a semiconductor surface," *Surf. Sci.*, vol. 175, no. 2, pp. 415–420, 1986.

[3] J. G. Simmons, "Generalized Formula for the Electric Tunnel Effect between Similar Electrodes Separated by a Thin Insulating Film," *J. Appl. Phys.*, vol. 34, no. 6, pp. 1793–1803, 1963.

[4] N. D. Jäger, Ph. Ebert, K. Urban, R. Krause-Rehberg, and E. R. Weber, "Scanning tunneling microscopy and spectroscopy of semi-insulating GaAs," *Phys. Rev. B*, vol. 65, p. 195318, May 2002.

[5] N. D. Jäger, E. R. Weber, K. Urban, and Ph. Ebert, "Importance of carrier dynamics and conservation of momentum in atom-selective STM imaging and band gap determination of GaAs(110)," *Phys. Rev. B*, vol. 67, p. 165327, 4 2003.

[6] R. M. Feenstra, "Electrostatic Potential for a Hyperbolic Probe Tip near a Semiconductor," *J. Vac. Sci. Technol. B*, vol. 21, no. 5, pp. 2080–2088, 2003.

[7] R. Seiwatz and M. Green, "Space Charge Calucations for Semiconductors," *J. Appl. Phys.*, vol. 29, pp. 1034–1040, 1958.

[8] R. Sauer, *Halbleiterphysik: Lehrbuch für Physiker und Ingenieure*. Oldenbourg Wissenschaftsverlag GmbH, 2009.

[9] S. M. Sze and K. K. Ng, *Physics of Semiconductor Devices*. New York: Wiley-Interscience, 3 ed., 2007.

[10] J. S. Blakemore, "Approximations for Fermi-Dirac integrals, especially the function $F_{1/2}(\eta)$ used to describe electron density in a semiconductor," *Solid-State Electronics*, vol. 25, no. 11, pp. 1067–1076, 1982.

[11] N. D. Jäger, *Effects of individual dopant atoms on the electronic properties of GaAs investigated by scanning tunneling microscopy and spectroscopy.* No. 4053 in Berichte des Forschungszentrum Jülich, Jülich: Forschungszentrum Jülich GmbH, 2003.

[12] R. M. Feenstra, "Tunneling spectroscopy of the (110) surface of direct-gap III-V semiconductors," *Phys. Rev. B*, vol. 50, pp. 4561–4570, Aug 1994.

[13] M. Schnedler, V. Portz, P. H. Weidlich, R. E. Dunin-Borkowski, and P. Ebert, "Quantitative description of photoexcited scanning tunneling spectroscopy and its application to the GaAs(110) surface," *Phys. Rev. B*, vol. 91, p. 235305, Jun 2015.

[14] S. Selberherr, *Analysis and Simulation of Semiconductor Devices.* Vienna, New York: Springer, 1984.

[15] R. M. Feenstra, Y. Dong, M. P. Semtsiv, and W. T. Masselink, "Influence of Tip-induced Band Bending on Tunneling Spectra of Semiconductor Surfaces," *Nanotechnol.*, vol. 18, p. 044015, 2007.

[16] H. C. Casey, D. D. Sell, and K. W. Wecht, "Concentration dependence of the absorption coefficient for n- and p-type GaAs between 1.3 and 1.6 eV," *J. Appl. Phys.*, vol. 46, no. 1, pp. 250–257, 1975.

[17] R. A. Smith, *Semiconductors.* Cambridge: Cambridge University Press, 1959.

[18] J. R. Chelikowsky and M. L. Cohen, "Nonlocal pseudopotential calculations for the electronic structure of eleven diamond and zinc-blende semiconductors," *Phys. Rev. B*, vol. 14, pp. 556–582, Jul 1976.

[19] J. R. Chelikowsky and M. L. Cohen, "Erratum: Nonlocal pseudopotential calculations for the electronic structure of eleven diamond and zinc-blende semiconductors," *Phys. Rev. B*, vol. 30, p. 4828, Oct 1984.